Journal of Comparative Physiology A

Optic lobe organization in stomatopod crustacean species having different degrees of retinal complexity

--Manuscript Draft--

Manuscript Number:	
Full Title:	Optic lobe organization in stomatopod crustacean species having different degrees of retinal complexity
Article Type:	S.I. : Visual Circuits
Funding Information:	Air Force Office of Scientific Research (FA9550-18-1-0278) — Dr. Thomas W Cronin
Abstract:	Stomatopod crustaceans possess tripartite compound eyes; upper and lower hemispheres are separated by an equatorial midband of several ommatidial rows. The organization of stomatopod retinas is well studied, but their optic lobes are less understood. We used histological staining, immunolabeling, and fluorescent tracer injections to compare optic lobes in two 6-midband-row species, Neogonodactylus oerstedii and Pseudosquilla ciliata , to those in two 2-midband-row species, Squilla empusa and Alima pacifica . Compared to the 6-row species, we found structural simplification in all optic neuropils in both 2-row species. Photoreceptor axons from 2-row midband ommatidia supply two sets of enlarged lamina cartridges, but a gap in the lamina exists at the location where the cartridges of the dorsal four ommatidial rows of 6-row species would appear. The tripartite arrangement and enlarged axonal projections from the two rows of midband ommatidia can be traced throughout the entire optic lobe, but other details of both medullar and lobular neuropils found in 6-row species are lacking. Our results support the hypothesis that 2-row midband species are derived from an 6-row ancestor, and suggest that specializations in the deep medulla and lobula found solely in 6-row species are important for color and polarization analysis.
Corresponding Author:	Thomas W Cronin University of Maryland Baltimore County Baltimore, Maryland United States
Corresponding Author Secondary Information:	
Corresponding Author's Institution:	University of Maryland Baltimore County
Corresponding Author's Secondary Institution:	
First Author:	Thomas W Cronin
First Author Secondary Information:	
Order of Authors:	Thomas W Cronin Chan Lin, PhD Alice Chou, BS
Order of Authors Secondary Information:	
Author Comments:	This paper is for the special issue on "Visual Circuits in Arthropod Brains"
Suggested Reviewers:	

Optic lobe organization in stomatopod crustacean species having different degrees of retinal complexity

Chan Lin[1,2], Alice Chou[1] and Thomas W. Cronin[1]

[1] Department of Biological Sciences, University of Maryland Baltimore County, Baltimore, Maryland 21250

[2] Department of Invertebrate Zoology, Smithsonian National Museum of Natural History, Washington, D.C. 20560

Supporting Grant: Air Force Office of Scientific Research (FA9550-18-1-0278)

ABSTRACT

Stomatopod crustaceans possess tripartite compound eyes; upper and lower hemispheres are separated by an equatorial midband of several ommatidial rows. The organization of stomatopod retinas is well studied, but their optic lobes are less understood. We used histological staining, immunolabeling, and fluorescent tracer injections to compare optic lobes in two 6 midband-row species, *Neogonodactylus oerstedii* and *Pseudosquilla ciliata*, to those in two 2-midband-row species, *Squilla empusa* and *Alima pacifica*. Compared to the 6-row species, we found structural simplification in all optic neuropils in both 2-row species. Photoreceptor axons from 2-row midband ommatidia supply two sets of enlarged lamina cartridges, but a gap in the lamina exists at the location where the cartridges of the dorsal four ommatidial rows of 6-row species would appear. The tripartite arrangement and enlarged axonal projections from the two rows of midband ommatidia can be traced throughout the entire optic lobe, but other details of both medullar and lobular neuropils found in 6-row species are lacking. Our results support the hypothesis that 2-row midband species are derived from a 6-row ancestor, and suggest that specializations in the deep medulla and lobula found solely in 6-row species are important for color and polarization analysis.

KEYWORDS

Stomatopoda; compound eye; visual system; neuroanatomy; vision

INTRODUCTION

Stomatopod crustaceans, known commonly as mantis shrimps, are predatory marine invertebrates considered to possess some of the most complex visual systems known to biologists, being capable of color vision, ultraviolet vision, motion vision, and both linear and circular polarization vision (Bok et al. 2015; Chiou et al. 2008; Cronin and Marshall 1989a; Cronin et al. 1994; 2003; Kleinlogel and Marshall 2006; Marshall and Oberwinkler 1999; Marshall 1988; Marshall et al. 1991a,b; 1996; 1999). Approximately 400 described species of this order inhabit a diversity of photic environments, most in shallow, tropical waters, and display a variety of eye designs (Harling 2000; Manning et al. 1984; Marshall et al. 1991a,b). Comprised of thousands of ommatidia, their apposition compound eyes are divided into three regions with overlapping visual fields (Fig. 1): the upper and lower hemispheres, and a specialized midband region dividing the two (Cronin 1986; Exner 1891; Horridge 1978; Marshall and Land 1993a,b; Marshall et al. 1991a,b).

The upper and lower hemispheres are structured much like the eyes of typical malacostracan crustaceans and are thought to encode luminance, linear polarization information, and spatial vision (Cronin and Marshall 2004; Marshall et al. 1991a; 2007). The rhabdoms here are split into two tiers, consisting of a distal R8 cell and the underlying fused R1-R7 cells.

The equatorial midband is more complicated, comprised of two, three, or six parallel rows of enlarged ommatidia (Harling 2000; Manning et al. 1984; Marshall 1988; Marshall et al. 1991a). Modifications within midband ommatidia produce the very unusual color vision system characteristic of stomatopods. In four stomatopod superfamilies (Gonodactyloidea, Lysiosquilloidea, Pseudosquilloidea, and Hemisquilloidea), the midband is comprised of six ommatidial rows, within which up to

14 morphologically and functionally distinct photoreceptor classes have been documented (Cronin and Marshall 1989a,b; Cronin et al. 1994; Marshall and Oberwinkler 1999; Marshall 1988; Marshall et al. 1991a,b). The rhabdoms of midband rows 1-4 are uniquely arranged into three distinct tiers formed by subsets of photoreceptors. This arrangement, together with a system of filtering pigments in rows 2 and 3, allows absorbance of different parts of the color spectrum by the different photoreceptor subsets as the light passes through the entire length of the rhabdom (Cronin et al. 2014; Cronin and Marshall 1989a,b; Marshall et al. 1991b). Surprisingly, despite the numerous color channels found in 6 midband-row species, these animals perform poorly in behavioral wavelength discrimination tests (Thoen et al. 2014). In midband rows 5 and 6, the distal photoreceptor R8 cells detect linear polarized light in the UV range and serve as a quarter-wave retarder for the underlying photoreceptors R1-7, allowing them to detect circularly polarized light (Chiou et al. 2008; Roberts et al. 2009).

Unlike the animals just described, species of the superfamily Squilloidea, which often live in deeper or more turbid habitats, possess only two midband rows and show no sign of color vision (Cronin 1985; Cronin et al. 1993; Exner 1891; Marshall et al. 1991a; Schiff 1963). Phylogenetic analyses suggest that this decreased visual complexity is an evolutionary loss (Ahyong and Harling 2000; Ahyong and Jarman 2009; Harling 2000; Porter et al. 2010; 2013). Uniquely, the visual adaptations found in the hemispheres are also found in the two midband rows.

Given the unique visual features of these peculiar animals, how do they process parallel channels of visual information? In malacostracan crustaceans, visual information from photoreceptors is relayed to the central brain through a series of retinotopically

arranged optic neuropils situated within the eyestalk. These neuropils include, distally to proximally, the lamina, medulla, and lobula, and a small lobula plate located posterior to the lobula (Strausfeld 2005; Strausfeld et al. 2016). Similar to the ground-pattern organization of malacostracan optic lobes, the stomatopod lamina, medulla, and lobula are connected sequentially by axons through two optic chiasmata, while the lobula plate is linked by uncrossed axons originating in the medulla and lobula (Kleinlogel and Marshall 2005; Kleinlogel et al. 2003; Thoen et al. 2017). Notably, visual information descending from the midband area of stomatopods with 6-row midbands is segregated and processed through optic neuropils with a series of anatomical elaborations. These include six enlarged lamina cartridges, corresponding to each of the six ommatidial rows, and a hernia-like expansion in the midlines of the medulla and lobula (Kleinlogel and Marshall 2005; Kleinlogel et al. 2003; Thoen et al. 2017; 2018). Developmentally, unlike all other crustaceans, during larval metamorphosis to the juvenile adult, a brand new adult compound eye and a complete set of adult optic neuropils develop adjacent to the larval eye and larval neuropils (Cronin et al. 2017; Lin and Cronin 2018). After metamorphosis, the larval eyes and optic neuropils degenerate and are completely replaced by the adult system (Lin and Cronin 2018). This unique stomatopod optic lobe structure, which accommodates a drastic number of parallel information channels, represents an evolutionary innovation.

Here, we provide a detailed study comparing the optic lobes in two 6 midband-row species, *Neogonodactylus oerstedii* and *Pseudosquilla ciliata*, to the optic lobes in two 2 midband-row species, *Squilla empusa* and *Alima pacifica*. By doing so, we aim to provide insight regarding the underlying principles of visual processing in all stomatopod

crustaceans, and we hope to learn how the optic lobes of 2-row and 6-row species differ. This is particularly interesting, given that the squilloids appear to have been derived from an ancestor with a 6-row midband.

MATERIALS AND METHODS

Animals

Stomatopod species *S. empusa*, *N. oerstedii* and *P. ciliata* were collected in the Florida Keys, USA. *A. pacifica* were collected at Lizard Island Research Station near the Australia's Great Barrier Reef (Great Barrier Reef Marine Park Authority Permit no. G12/35005.1, Fisheries Act no. 140763).

Osmium-ethyl gallate staining

The staining procedures have previously been described (Lin and Cronin 2018). In brief, eyestalk tissue was fixed in cacodylate fixative (2% glutaraldehyde, 1% paraformaldehyde in 0.16M sodium cacodylate buffer) with 10% sucrose at 4°C overnight. After several washes in cacodylate buffer, tissue was immersed in 1% osmium tetroxide in the dark with continuous agitation for 2.5h at 4°C and an additional 1.5h at room temperature. After several washes in buffer, tissue was put in a second immersion with supersaturated ethyl gallate (~1% in distilled water) in the dark with continuous agitation for 1.5h at 4°C and an additional 30 min at room temperature. After several washes in distilled water, tissue was dehydrated, transferred into Durcupan plastic (Sigma, St. Louis, MO) via propylene-oxide, and polymerized at 65°C. Blocks were

serially sectioned at 20-30 μm. Sections were mounted with Permount (Electron Microscopy Science, Hatfield, PA) and coverslipped for light microscopy.

Bodian reduced silver staining

The eyestalk tissue was removed for silver staining following Bodian's original method (Bodian 1936). In brief, tissue was fixed in AAF (17 ml 100% ethanol, 1 ml glacial acetic acid, 2 ml 37% formaldehyde) overnight at 4°C, dehydrated in an ethanol series, cleared in terpineol, embedded in Paraplast Plus (Tyco, Mansfield, MA), and serially sectioned at 12 μm. Sections were arranged on glass slides, flattened by warming to 50°C, and then deparaffinized, rehydrated, and silver impregnated overnight at 60°C with 2.5 g Protargol-S (Polysciences, Warrington, PA), 250 ml ddH2O, and 6 g clean copper filings. The following day, tissue was developed in 1% hydroquinone and 2% sodium sulfite, toned in 1% gold chloride, differentiated in 2% oxalic acid, and fixed in 5% sodium thiosulfate. Tissue was dehydrated again in an ethanol series before being mounted with Entellan (Electron Microscopy Science, Hatfield, PA).

Golgi impregnations

Combined Golgi Colonnier and Golgi rapid procedures were used as described in Lin and Strausfeld (2012). In brief, twenty eyestalk tissues were dissected out under 2.5% potassium dichromate solution with 10% sucrose, then placed in 5 parts of this solution with 1 part of 25% glutaraldehyde and kept in complete darkness for 5 days at room temperature. Next, in preparation for the second chromation step, tissues were washed several times in 2.5% potassium dichromate solution (omitting sucrose) and then

incubated in 99 parts of 2.5% potassium dichromate solution with 1 part of 1% osmium tetroxide for 3 days at room temperature. Tissues were then washed several times in 0.75% silver nitrate solution in distilled water and left in this solution for 3 days. Finally, tissues were washed in distilled water, dehydrated, transferred into Durcupan plastic (Sigma, St. Louis, MO) via propylene-oxide, and polymerized at 65°C. Blocks were serially sectioned at 25 μm. Sections were mounted with Permount (Electron Microscopy Science, Hatfield, PA) and coverslipped.

Immunolabeling

Eyestalk tissue was fixed overnight in 4% paraformaldehyde with 10% sucrose in phosphate buffer (pH 7.4), and then washed in phosphate buffered saline (PBS), embedded in albumin gelatin, and sectioned at 60 μm with a vibratome. After being washed with PBS-TX (0.5% Triton X-100 in PBS), sections were blocked in 5% normal goat serum (Vector Laboratories, Burlingame, CA) for 1 hr and then incubated overnight in monoclonal synapsin antiserum (SYNORF1: *Drosophila* synapsin I isoform; 1: 50; Developmental Studies Hybridoma Bank, University of Iowa, IA) and α-tubulin antiserum (1:1000; Abcam, Eugene, Oregon) on a shaker at room temperature. The following day, sections were washed with PBS-TX and incubated overnight in the secondary goat anti-mouse immunoglobulins conjugated to Alexa Fluor 633 (3:1000; Thermo Fisher Scientific, Waltham, MA) and goat anti-rabbit immunoglobulins conjugated to Alexa Fluor 555 (3:1000; Thermo Fisher Scientific). The following day, sections were washed with PBS, mounted on slides and coverslipped in a medium of 25% polyvinyl alcohol, 25% glycerol and 50% PBS.

Fluorescent tracer injections

Eyes from ten *S. empusa* individuals were used for tract tracing experiments. Each animal was anesthetized with ice and immobilized by attaching its back to a glass slide with Super Glue, so that the eyestalks were oriented above water for dye injections while the body and pleopods submerged in seawater. Pulled glass capillaries tipped with crystals of dextran-conjugated Texas Red (molecular weight 3,000 kDa, Thermo Fisher Scientific, Waltham, MA) were inserted into the eyestalk tissue targeting the midband pathway. The animals were kept alive overnight at room temperature to allow tracer uptake and diffusion through neurons. The eyestalk tissue was then dissected out and fixed in 4% paraformaldehyde in PBS with 10% sucrose overnight at 4°C, and then dehydrated, embedded in Spurr's plastic (Electron Microscopy Science, Hatfield, PA), serially sectioned at 20 μm, and mounted with Fluoromount (Crescent Chemical, Islandia, NY).

Image acquisition and image processing

Images of Golgi, Bodian, and osmium-ethyl gallate-stained preparations were collected using a Nikon digital camera D5100 with a T-mount NDPL-1 microscope camera adapter (AmScope, Irvine, CA) connected to an Olympus BH-2 microscope (Olympus, Tokyo, Japan). Images of stomatopod brains and eyestalks were collected with the same camera connected to a dissecting microscope. Fluorescent tracer, synapsin, and α-tubulin-labeled eyestalk tissues were imaged using a Leica SP5 laser scanning confocal microscope (Leica Microsystems, Buffalo Grove, IL). Image stacks were collected with a 10x/0.4 Plan Apochromat objective at 1,024 x 1,024 pixel resolution at approximately 1 μm depth

intervals. Selected images were adjusted for brightness and contrast using Adobe Photoshop CC 2015 (Adobe Systems, San Jose, CA).

RESULTS

In all staining results, the two 2-midband-row species *S. empusa* and *A. pacifica* show similar optic lobe morphologies, as do the two 6-midband-row species *N. oerstedii* and *P. ciliata*. Therefore, unless specifically noted, results described here for any single species are also true of the corresponding species of each eye type.

The morphology of stomatopod brains and optic lobes

Like many crustaceans with eyestalks, the stomatopod central brain is connected with neural tissue in the eyestalks through a thin connection (arrowheads, Fig. 1C, D), which consists of the optic nerves and numerous protocerebral tracts connecting the lateral protocerebrum and antennular olfactory lobe. The stomatopod eyestalk tissues are impressive in size; the tissue in each eyestalk alone is larger than the central brain (Fig. 1C, D). For both 2- and 6-midband-row species, the enlarged midband ommatidial facets and the tripartite arrangement of the eyes, which include upper and lower hemispheres (UH and LH) and the midband (MB) (Fig. 1 insets), manifest not only at the retina level (Fig. 1C, D), but also throughout the optic lobes (Fig. 2A, 3A).

Beneath the compound eyes, three primary optic neuropils were revealed with all stains used here. These include a planar lamina (LA), a dome-shaped medulla (ME), and a kidney-shaped lobula (LO) (Fig. 2, 3). A lobula plate exists posterior to the lobula (Thoen et al. 2017); however, this neuropil is minute in both the 2- and 6-midband-row

species and thus is not shown here. Each optic neuropil is composed of as many vertical columns as the number of ommatidia in the eye, as well as horizontal layers formed by stratified arrangements of synaptic networks between input and output neurons. Histological sectioning at the antero-posterior plane reveals the characteristic outer and inner optic chiasmata, where the outer optic chiasma connects the lamina and medulla (yellow arrowheads, Fig. 2B-D, and 3B) and the inner optic chiasma connects the medulla and lobula (yellow arrows, Fig. 2B-D, and 3B). Comparing the overall optic lobe morphology between 2-midband-row species (Fig. 2) and 6-midband-row species (Fig. 3) reveals that the 6-row species have relatively larger medullas and lobulas with more defined stratification layers. At least 11 medulla layers and 13 lobula layers can be resolved in *N. oerstedii* (Fig. 3B), compared to about 8 layers in the *S. empusa* medulla and lobula, respectively (Fig. 2 B-D).

The missing lamina cartridges and the unique midband representation in the optic lobes of 2-row species

In *S. empusa* and *A. pacifica*, photoreceptor axons from the two midband rows project to two lamina cartridges lying adjacent to the lower hemispheric lamina (yellow and white arrowheads, respectively, Fig. 4A). A wide space lacking lamina cartridges exists (bracket, Fig. 4A) at the location corresponding to the four lamina cartridges supplied by the four color-processing midband ommatidial rows in the 6-row species (1-4, Fig. 4B). This observation suggests that the two remaining midband rows in squilloids are derived from, and perhaps physiologically comparable to, the midband rows 5 and 6 polarization processing channels of stomatopods with 6-row midbands. Interestingly, the midband

lamina cartridges in 6-row species are at least twice the diameter of their hemispheric counterparts (compare 1-6 with white arrowheads, Fig. 4B), while in the 2-row species the two midband lamina cartridges are only slightly larger than those hemispheric ones (compare yellow arrowheads with white arrowheads, Fig. 4A).

The relationship between the midband rows of the 2-row and 6-row species is further confirmed by the innervation pattern at the distal margin of the optic lobes. Here, a prominent axonal tract runs through the midline and separates the lamina and medulla into two halves (Fig. 4C, D). Photoreceptor axons from the two midband rows in the 2-row species project to the lower halves of the lamina (yellow arrowheads, Fig. 4C), as do those of the rows 5 and 6 in the 6-row species (5, 6, Fig. 4D). Axons from rows 1-4 in the 6-row species, on the other hand, project to the upper half (1-4, Fig. 4D).

Axons from the midband lamina cartridges project to a distinct hernia-like outswelling at the distal surface of the medulla of both 6-row species (yellow arrow, Fig. 4B), whereas no obvious medulla extension exists associated with the midband in the 2-row species (Fig. 4A). Nevertheless, a hernia-like midband outswelling is found at the distal surface of the lobula in both 2-row species (yellow arrows, Fig. 3E-G). This observation suggests that neither the enlarged midband tracts (white arrowheads, Fig. 4E-G) nor the distinct midband representation in the optic neuropil (i.e. the outswelling, yellow arrows, Fig. 4E-G) are involved solely with color processing in stomatopods, as those neural specializations also exist in stomatopod species without color vision.

<u>Distinct midband outputs in the 2-row species</u>

The midband projection pattern in the 2-row species was further investigated using a combination of neuroanatomical methods to provide a direct comparison with results from 6 midband-row species that have been recently published (Thoen et al. 2017; 2018). Bodian reduced silver staining again reveals a pair of slightly larger midband lamina cartridges (yellow arrowheads, Fig. 5A), compared to their counterparts in the hemispheres (white arrowheads, Fig. 5A), and their associated darkly stained output tracts in the medulla (arrowhead, Fig. 5B) and lobula (arrowhead, Fig. 5C). These darkly stained output axons have accumulated more silver in the staining process than the axons of outputs from the hemispheres, indicating that they are larger or thicker in size. This result is also shown in the immunostained preparations with antibodies raised against synapsin and α-tubulin (arrowheads, Fig. 5D and 5E, respectively). To further reveal the detailed arborization patterns of these midband outputs, direct fluorescent tracer injections targeting the midband lamina, as well as Golgi impregnations were used. Results show that these midband axonal outputs travel down faithfully within their own vertical columns in the medulla without sending lateral collaterals that cross into neighboring columns from ommatidia in the hemispheres (arrowheads, Fig 5F, G).

DISCUSSION

Comparing the optic lobe organization between 2- and 6-midband-row species

Previous studies on stomatopod species with 6-row midbands (including *Haptosquilla glyptocercus*, *H. trispinosa*, *Chorisquilla trigibbosa*, *Gonodactylus smithii*, *G. chiraga*, and *G. platysoma*) established that the midband is represented in the optic lobe by enlarged lamina cartridges, formed by larger midband photoreceptor terminals and

corresponding monopolar neurons than their hemispheric counterparts, and a hernia-like outswelling at the distal surface of the medulla and lobula (Kleinlogel and Marshall 2005; Kleinlogel et al. 2003; Thoen et al. 2017; 2018). Using osmium-ethyl gallate staining, we show similar results in the 6-midband-row species *N. oerstedii* and *P. ciliata* (Fig. 3A, 3B, 4B, 4D) and provide evidence that, in the 2-midband-row species *S. empusa* and *A. pacifica*, the missing four rows would correspond to midband rows 1-4, the color-processing channels in the 6-row species (Fig. 4A-D). This latter observation is consistent with the hypothesis that 2-row species are derived from an ancestor that had 6-row midbands (Ahyong and Harling 2000; Ahyong and Jarman 2009; Harling 2000; Porter et al. 2010; 2013), and suggests that the remaining two midband-rows in squilloids are likely homologous to the polarization-processing rows 5 and 6 of 6-row ancestors.

However, several features in the eye distinguish squilloid midbands from rows 5 and 6 of 6-row species. First, squilloid midband ommatidia often lack the distal R8 cells that are sensitive to ultraviolet and linearly polarized light in rows 5 and 6 of 6-row species (Kleinlogel and Marshall 2006; Marshall and Oberwinkler 1999; Marshall et al. 1991a; Schönenberger 1977). Second, only one spectral class of photoreceptors exists in the squilloid midband, whose opsin expression pattern is thought to be found throughout the entire squilloid eye (Cronin et al. 1993; Valdez-Lopez et al. 2018), whereas unique photoreceptor classes and visual pigments are found in the rows 5 and 6 of 6-row species (Cronin et al. 1996; Marshall 1988; Marshall et al. 1991a,b).

Compared to 6-row species, the midband lamina cartridges in the 2-row species are not drastically enlarged compared to the lamina cartridges of the dorsal and ventral hemispheres (Fig. 4A, 5A), but the axonal projections associated with the midband

remain distinct from those arriving from ommatidia of the hemispheres (Fig. 2A, 4E-G, 5D, E) and are more darkly stained in the Bodian preparations than axons from the hemispheres (Fig. 5A-C). This is likely a case of keeping the ancestral state character (plesiomorphy) without functional significance, as the photoreceptor types and arrangements of the 2-row midbands in squilloids are nearly identical to those in the hemispheres (Cronin 1985; Cronin et al. 1993; Marshall et al. 1991a), and no midband specialized hernia-like swelling is found in squilloid medullas (Fig. 2A, 4A). However, we describe a previously unidentified swelling associated with midband projections along the distal surface of squilloid lobulas (Fig. 4E-G). This small lobula expansion might, again, be a plesiomorphic character that is common to all stomatopods (Kleinlogel and Marshall 2005; Kleinlogel et al. 2003). Whether or not this squilloid lobula hernia has any functional significance awaits further investigation.

Potential neural substrate for color processing in stomatopods

A recent study described the detailed organization of the midband representation in the medulla and lobula of the 6-row species *G. smithii* and proposed a potential neural substrate for cross-talk between the color-, polarized light-, and luminance-processing channels (Thoen et al. 2018). In *G. smithii*, midband inputs to the deep layers of medulla send out collaterals that extend across neighbor columns serving hemispheric ommatidia that view a strip of the visual scene about 10 degrees above and below the midband (Thoen et al., 2018). In the deep layers of the *G. smithii* lobula, likewise, two distinct bundles of midband axonal tracts, corresponding to the color and circular-polarization retinal channels, respectively, send out collaterals that intersect the entire set of upper and

lower columns descending from the hemispheres (Thoen et al. 2018). In *S. empusa* and *A. pacifica*, we found fewer medulla and lobula layers than we observed in *N. oerstedii* and *P. ciliata* (compare Fig. 2B-D with Fig. 3B). As these layers are composed of stratified arrangements of synaptic networks formed by distinct axon terminals of input neurons and dendritic processes of output neurons, greater numbers of layers in the medulla and lobula indicate a greater neuronal complexity and diversity in animals with 6-row midbands. Compared to squilloids, these extra layers in the deep medulla and lobula of 6-row species likely provide neural substrates for processing color or circularly polarized light information descending from the additional midband ommatidia. In contrast, numerous fluorescent tracer injections and Golgi impregnations failed to reveal midband projections with widespreading collaterals extending to neighboring columns in 2-row species (Fig. 5F, 5G). Therefore, our data support Thoen et al.'s (2017; 2018) hypothesis that specialized Y-shaped neurons in the deep medulla and lobula of stomatopod species with 6-row midbands play a role in color and polarization signal integration.

In conclusion, by comparing the optic lobe organization between stomatopod species with 2- and 6-row midbands, we found that the tripartite arrangement of the eye, which includes upper and lower hemispheres and the midband as well as enlarged axonal projections associated with midband ommatidia, is well conserved throughout the optic lobes and likely represents a common specialization across all stomatopods. Compared to the 6-row species, we also found evidence of structural simplification in all three optic neuropils in the 2-row species. These including a lamina gap and a structurally simplified medulla and lobula. The extra layers and specialized cross-columnar neurons exclusively

found in the medulla and lobula of 6-row species thus provide a promising target for future studies on color processing in stomatopods.

ACKNOWLEDGEMENTS

We are grateful to Michael Bok for the image for Figure 1B. This work was supported by the Air Force Office of Scientific Research under grant number FA9550-18-1-0278.

CONFLICT OF INTEREST

The authors have no conflicts of interest to declare.

REFERENCE LIST

Ahyong ST, Harling C (2000) The phylogeny of the stomatopod Crustacea. Aust J Zool 48:607-642.

Ahyong ST, Jarman SN (2009) Stomatopod interrelationships: preliminary results based on analysis of three molecular loci. Arthropod Syst Phylogeny 67:91-98.

Bodian D (1936) A new method for staining nerve fibers and nerve endings in mounted paraffin sections. Anat Rec 65:89-97.

Bok MJ, Porter ML, Cronin TW (2015) Ultraviolet filters in stomatopod crustaceans: diversity, ecology and evolution. J Exp Biol 218:2055-2066.

Chiou TH, Kleinlogel S, Cronin T, Caldwell R, Loeffler B, Siddiqi A, Goldizen A, Marshall J (2008) Circular polarization vision in a stomatopod crustacean. Curr Biol 18:429-434.

Cronin TW (1985) The visual pigment of a stomatopod crustacean, *Squilla empusa*. J Comp Physiol A 156:679-687.

Cronin TW (1986) Optical design and evolutionary adaptation in crustacean compound eyes. J Crust Biol 6:1-23.

Cronin TW, Bok MJ, Lin C (2017) Crustacean larvae – vision in the plankton. Integr Comp Biol 57:1139-1150.

Cronin TW, Bok MJ, Marshall NJ, Caldwell RL (2014) Filtering and polychromatic vision in mantis shrimps: themes in visible and ultraviolet vision. Phil Trans R Soc B 369:20130032.

Cronin TW, Marshall J (2004) The unique visual world of mantis shrimps. In: Prete F (ed) Complex Worlds From Simpler Nervous Systems. MIT Press, Cambridge, MA, pp 239-268.

Cronin TW, Marshall NJ (1989a) Multiple spectral classes of photoreceptors in the retinas of gonodactyloid stomatopod crustaceans. J Comp Physiol A 166:261-275.

Cronin TW, Marshall NJ (1989b) A retina with at least ten spectral types of photoreceptors in a stomatopod crustacean. Nature 339:137-140.

Cronin TW, Marshall NJ, Caldwell RL (1993) Photoreceptor spectral diversity in the retinas of squilloid and lysiosquilloid stomatopod crustaceans. J Comp Physiol A 172:339-350.

Cronin TW, Marshall NJ, Caldwell RL (1996) Visual pigment diversity in two genera of mantis shrimps implies rapid evolution. J Comp Physiol A 179:371-384.

Cronin TW, Marshall NJ, Quinn CA, King CA (1994) Ultraviolet photoreception in mantis shrimp. Vision Res 34:1443-1449.

Cronin TW, Shashar N, Caldwell RL, Marshall J, Cheroske AG, Chiou TH (2003) Polarization vision and its role in biological signaling. Integr Comp Biol 43:549-558.

Exner S (1891) Die physiologie der facettierten augen von krebsen und insekten. Deuticke, Leipzig.

Harling C (2000) Reexamination of eye design in the classification of stomatopod crustaceans. J Crust Biol 20:172-185.

Horridge GA (1978) The separation of visual axes in apposition compound eyes. Phil Trans R Soc B 285:1-59.

Kleinlogel S, Marshall NJ (2005) Photoreceptor projection and termination pattern in the lamina of gonodactyloid stomatopods (mantis shrimp). Cell Tissue Res 321:273-284.

Kleinlogel S, Marshall NJ (2006) Electrophysiological evidence for linear polarization sensitivity in the compound eyes of the stomatopod crustacean *Gonodactylus chiragra*. J Exp Biol 209:4262-4272.

Kleinlogel S, Marshall NJ, Horwood JM, Land MF (2003) Neuroarchitecture of the color and polarization vision system of the stomatopod *Haptosquilla*. J Comp Neurol 467:326-342.

Lin C, Cronin TW (2018) Two visual systems in one eyestalk: the unusual optic lobe metamorphosis in the stomatopod *Alima pacifica*. Dev Neurobiol 78:3-14.

Lin C, Strausfeld NJ (2012) Visual inputs to the mushroom body calyces of the whirligig beetle *Dineutus sublineatus*: modality switching in an insect. J Comp Neurol 520:2562-2574.

Manning RB, Schiff H, Abbott BC (1984) Eye structure and the clasification of stomatopod crustacea. Zool Scripta 13:41-44.

Marshall J, Cronin TW, Kleinlogel S (2007) Stomatopod eye structure and function: a review. Arthropod Struct Dev 36:420-448.

Marshall J, Cronin TW, Shashar N, Land M (1999) Behavioural evidence for polarisation vision in stomatopods reveals a potential channel for communication. Curr Biol 9:755-758.

Marshall J, Oberwinkler J (1999) The colourful world of the mantis shrimp. Nature 401:873-874.

Marshall NJ (1988) A unique colour and polarization vision system in mantis shrimps. Nature 333:557-560.

Marshall NJ, Jones JP, Cronin TW (1996) Behavioural evidence for colour vision in stomatopod crustaceans. J Comp Physiol A 179:473-481.

Marshall NJ, Land MF (1993a) Some optical features of the eyes of stomatopods. I. eye shape, optical axes and resolution. J Comp Physiol A 173:565-582.

Marshall NJ, Land MF (1993b) Some optical features of the eyes of stomatopods. II. Ommatidial design, sensitivity and habitat. J Comp Physiol A 173:583-594.

Marshall NJ, Land MF, King CA, Cronin TW (1991a) The compound eyes of mantis shrimps (Crustacea, Hoplocarida, Stomatopoda). I. Compound eye structure: the detection of polarized light. Phil Trans R Soc B 334:33-56.

Marshall NJ, Land MF, King CA, Cronin TW (1991b) The compound eyes of mantis shrimps (Crustacea, Hoplocarida, Stomatopoda). II. Colour pigments in the eyes

of stomatopod crustaceans: Polychromatic vision by serial and lateral filtering. Phil Trans R Soc B 334:57-84.

Porter ML, Speiser DI, Zaharoff AK, Caldwell RL, Cronin TW, Oakley TH (2013) The evolution of complexity in the visual systems of stomatopods: insights from transcriptomics. Integr Comp Biol 53:39-49.

Porter ML, Zhang Y, Desai S, Caldwell RL, Cronin TW (2010) Evolution of anatomical and physiological specialization in the compound eyes of stomatopod crustaceans. J Exp Biol 213:3473-3486.

Roberts NW, Chiou T-S, Marshall NJ, Cronin TW (2009) A biological quarter-wave retarder with excellent achromaticity in the visible wavelength region. Nature Photonics 11:641-644.

Schiff H (1963) Dim light vision of *Squilla mantis*. Am J Physiol 205:927-940.

Schönenberger N (1977) The fine structure of the compound eye of *Squilla mantis* (Crustacea, Stomatopoda). Cell Tissue Res 176:205-233.

Strausfeld NJ (2005) The evolution of crustacean and insect optic lobes and the origins of chiasmata. Arthropod Struct Dev 34:235-256.

Strausfeld NJ, Ma X, Edgecombe GD, Fortey RA, Land MF, Liu Y, Cong P, Hou X (2016) Arthropod eyes: the early Cambrian fossil record and divergent evolution of visual systems. Arthropod Struct Dev 45:152-172.

Thoen HH, How MJ, Chiou TH, Marshall J (2014) A different form of color vision in mantis shrimp. Science 343:411-413.

Thoen HH, Sayre ME, Marshall J, Strausfeld NJ (2018) Representation of the stomatopod's retinal midband in the optic lobes: putative neural substrates for

integrating chromatic, achromatic and polarization information. J Comp Neurol 526:1148-1165.

Thoen HH, Strausfeld NJ, Marshall J (2017) Neural organization of afferent pathways from the stomatopod compound eye. J Comp Neurol 525:3010-3030.

Valdez-Lopez JC, Donohue MW, Bok MJ, Wolf J, Cronin TW, Porter ML (2018) Sequence, structure, and expression of opsins in the monochromatic stomatopod *Squilla empusa*. Integr Comp Biol 58:386-397.

FIGURE LEGENDS

Fig. 1 (**A**) *Squilla empusa*, a stomatopod species with a 2-row midband. (**B**) *Pseudosquilla ciliata*, which has a 6-row midband. (**C**) and (**D**) The eyestalk tissues and central brains of these two stomatopod species, respectively. Arrows indicate the thin neural connections between the two eyestalk tissues and the central brain. Insets: the compound eye morphology of these two species, respectively, each with a midband (MB) area separating the eye into upper and lower hemispheres (UH and LH). OL, optic lobe; CB, central brain (photograph in B, courtesy of Michael Bok).

F**ig. 2** Overall morphology of the optic lobes in the 2-row-midband species, *S. empusa*. (**A**) Osmium-ethyl gallate-stained frontal optic lobe sections showing the successive optic neuropil lamina (LA), medulla (ME), and lobula (LO). White arrowheads indicate the distinct midband axon projections through the medulla and lobula. (**B**)-(**D**) Bodian-stained horizontal optic lobe sections showing the optic neuropils and the characteristic outer optic chiasma (yellow arrowheads) between lamina and medulla, and the inner

optic chiasma (yellow arrows) between the medulla and lobula. UH, upper hemisphere; MB, midband; LH, lower hemisphere. Scale bars = 200 μm in **A** and **D**. Panels **B**-**D** are at the same magnification.

Fig. 3 Overall morphology of the optic lobes in the 6-row-midband species, *N. oerstedii*. Osmium-ethyl gallate-stained frontal (**A**) and horizontal (**B**) optic lobe sections showing the successive optic neuropil lamina (LA), medulla (ME), and lobula (LO) and the outer and inner optic chiasma (yellow arrowhead and arrow, respectively). White arrowheads indicate the distinct midband axon projections through the medulla and lobula. Scale bars = 100 μm.

F**ig. 4** Two-row midband species have lost their color processing channels. (**A**) Photoreceptor axons from the two midband rows supply two slightly enlarged lamina cartridges (yellow arrowheads) lying adjacent to the lamina cartridges of the lower hemisphere (white arrowheads). A gap (yellow bracket) in the lamina is present at the location of the missing lamina cartridges towards the upper side of the retina, corresponding to the locations of cartridges from the missing four rows of color-processing channels in the 6-midband-row species (1-4, **B**). Yellow arrow in (**B**) indicates the distinct medulla outswelling supplied by the 6-row-midband projections. At the distal margin of the stomatopod optic lobes, a prominent axonal tract runs through and separates the lamina and medulla into two halves (**C**), (**D**). Here, photoreceptor axons from the two midband rows project to the lower half (yellow arrowheads in **C**). This innervation pattern again corresponds with that of the rows five and six (5, 6 in **D**) in the

6-midband-row species, indicating the 2-row midband is homologous to midband rows 5 and 6 of 6-row species. (**E**)-(**G**) Distinct hernia-like outswelling (yellow arrows) associated with midband projections (arrowheads) in the 2-row species. (**A**), (**C**), (**E**) *S. empusa* frontal optic lobe sections. (**F**) *S. empusa* horizontal section. (**B**), (**D**) *P. ciliata* frontal sections. (**G**) *A. pacifica* frontal section. All panels are results of osmium-ethyl gallate stained preparations. LA, lamina; ME, medulla; LO, lobula. All scale bars = 100 μm.

Fig. 5 Distinct midband axonal projections that lack lateral axonal collaterals in the medulla and lobula of the 2-row species, *S. empusa*. (**A**)-(**C**) Midband lamina cartridges and axonal projections are larger in size and stain darker in Bodian reduced silver staining (arrowheads). (**D**), (**E**) Immunolabeled preparations with antibodies raised against synapsin and α-tubulin, respectively, also show these midband tracks in the medulla and lobula (arrowheads). (**F**) Fluorescent tracer injections and (**G**) Golgi preparations confirm that these midband axonal tracts travel within their vertical columns in the medulla without sending collaterals that cross into neighboring columns from ommatidia of the hemispheres (arrowheads showing the local axonal processes confined to the same vertical column, **F**, **G**). LA, lamina; ME, medulla; LO, lobula. Panels **A**-**C** and **D**, **E** are at the same magnification, respectively. Scale bars = 200 μm in **C** and **E,** and 50 μm in **F** and **G**.

Figure

Click here to access/download;Figure;Fig 1.tif

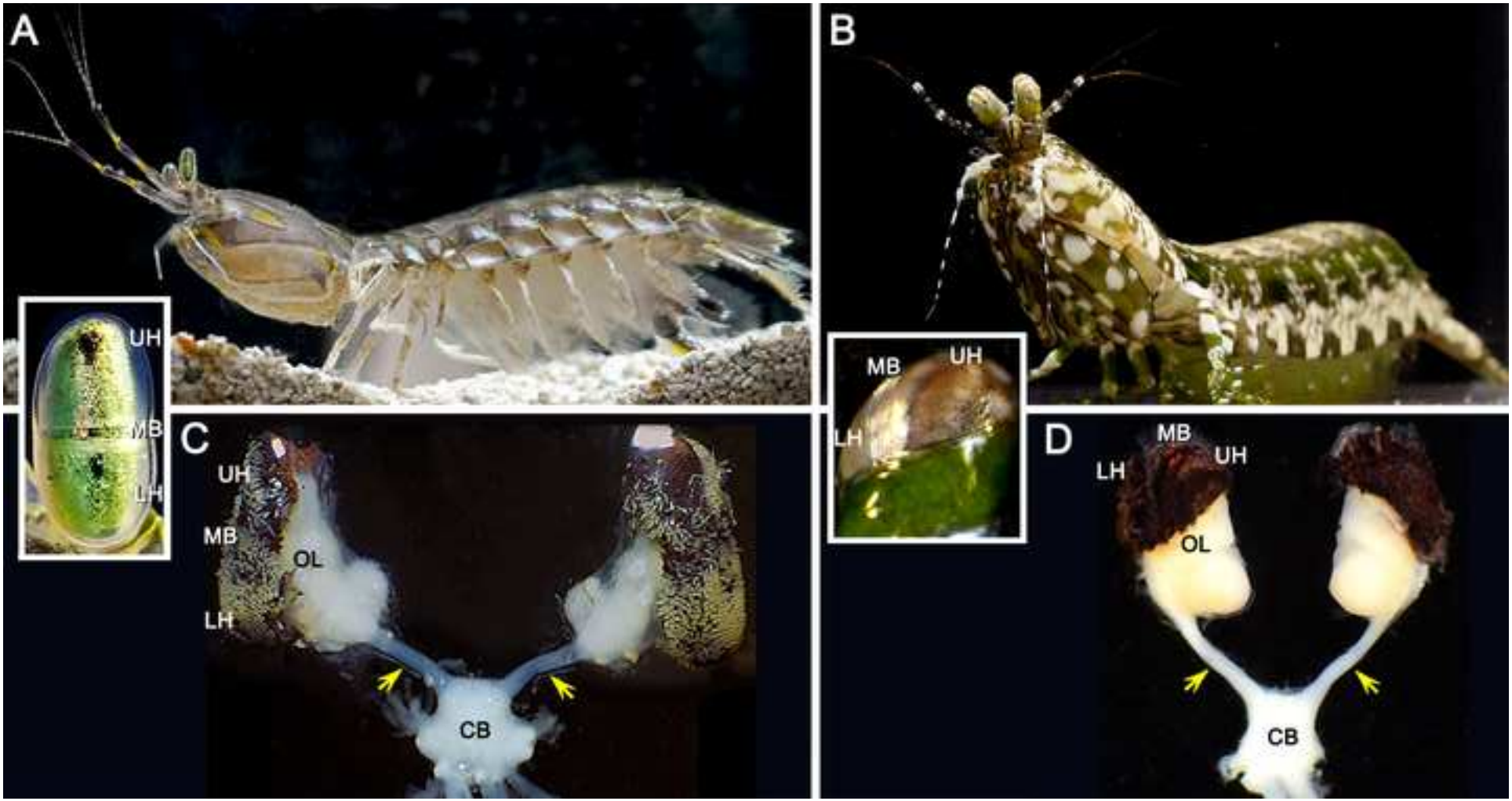

Figure

Click here to access/download;Figure;Fig 2.tif

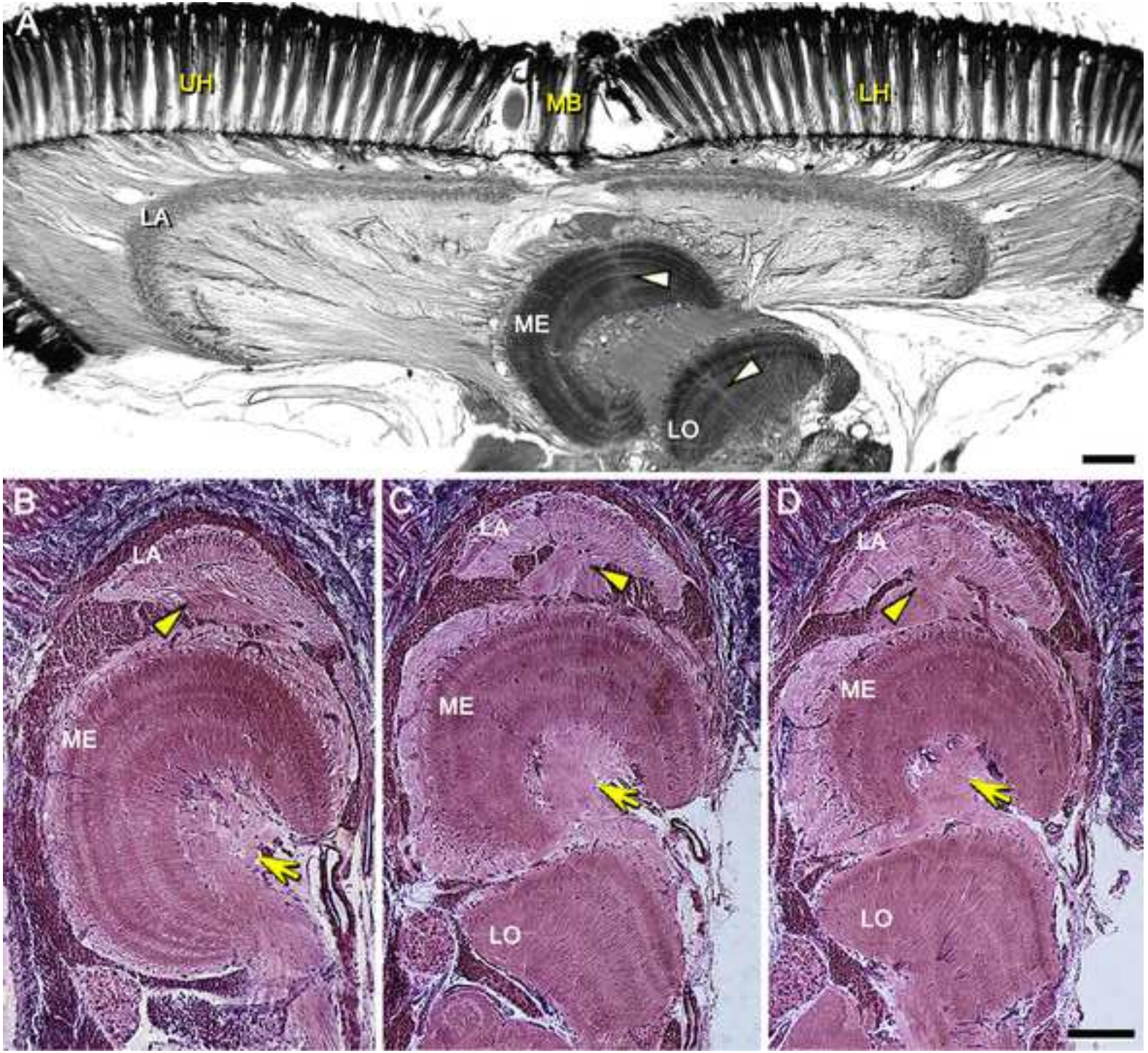

Figure

Click here to access/download;Figure;Fig 3.tif

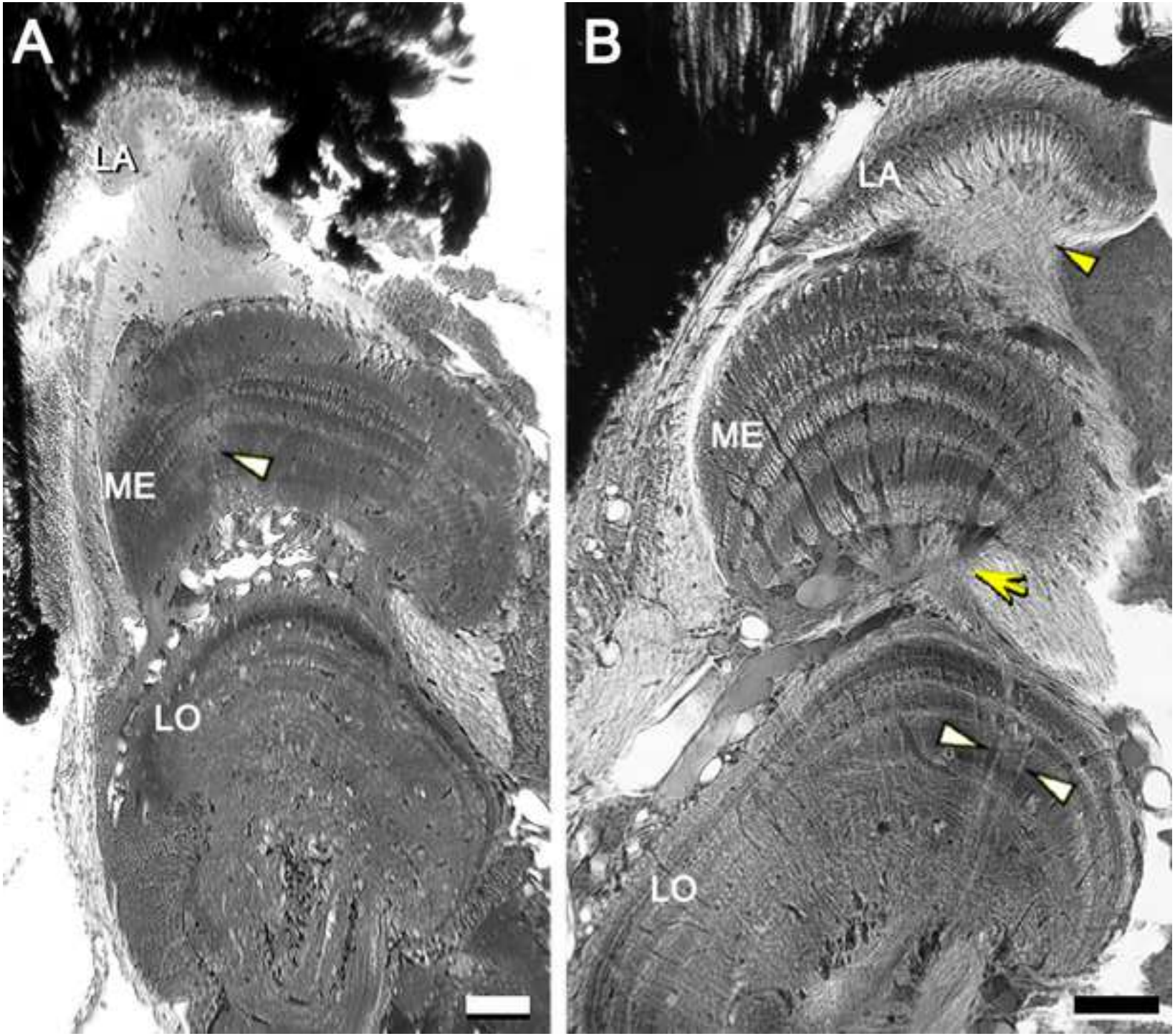

Figure

Click here to access/download;Figure;Fig 4.tif

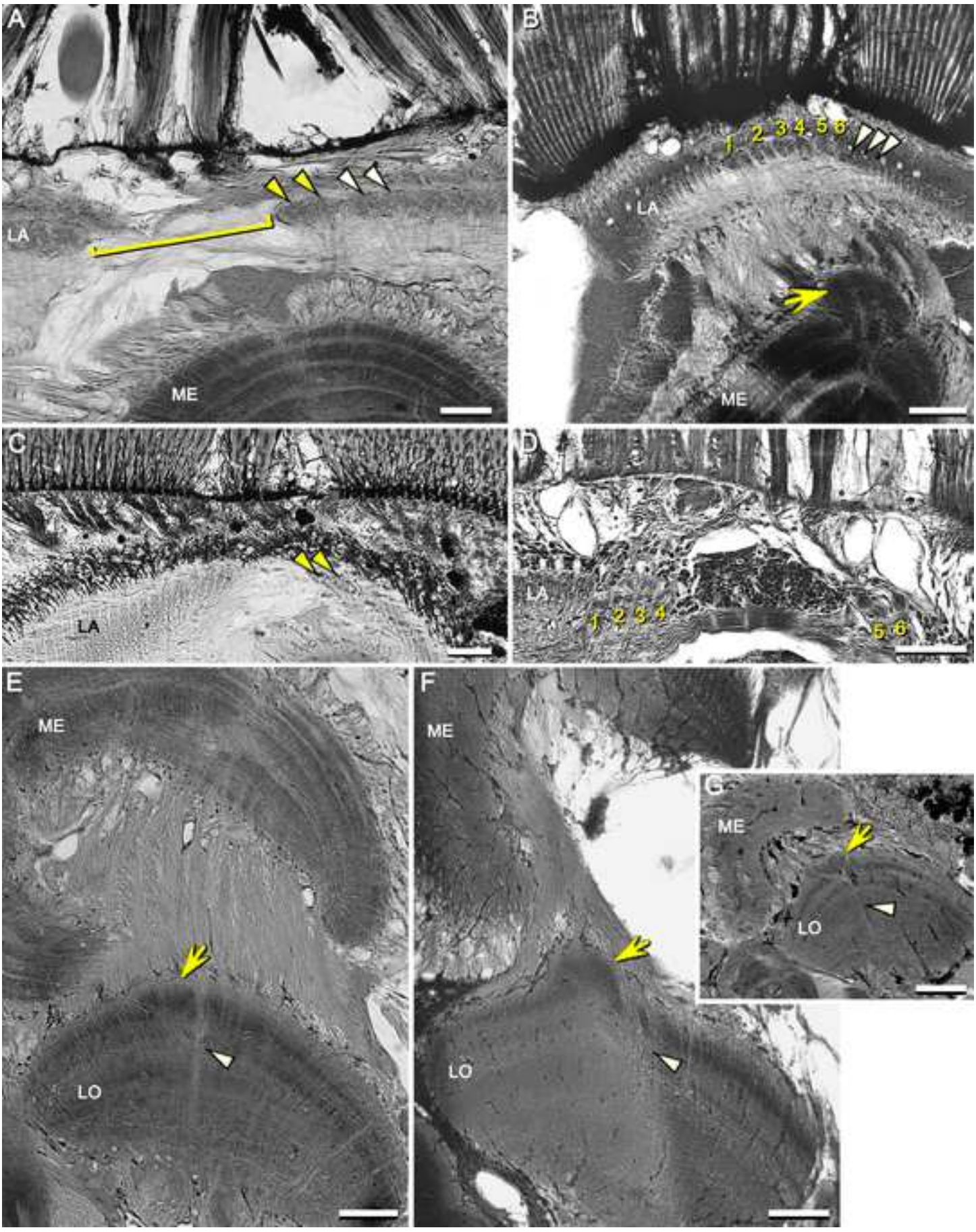

Figure

Click here to access/download;Figure;Fig 5.tif